ChemComm

Structural transition and chemical reactivity of atomic carbon chains

Journal:	*ChemComm*
Manuscript ID	CC-COM-04-2023-001711.R1
Article Type:	Communication

COMMUNICATION

Structural transition and chemical reactivity of atomic carbon chains

Received 00th January 20xx,
Accepted 00th January 20xx

DOI: 10.1039/x0xx00000x

Siyuan Fang,[a] Xiao Tong,[b] Dario Stacchiola,[b] and Yun Hang Hu[a]*

The sp-hybridized carbon chain (carbyne) is a representative 1D atomic material, whose bonding structure and chemical reactivity remain a mystery for a century. Here, we report the unexpected alternating bond orders of 1.4 and 2.6 for the most stable carbon chain and the *in-situ* diffuse reflectance infrared Fourier-transform spectroscopy (DRIFTS) detection of the temperature-dependent reversible change of the bond order alternation. Moreover, we revealed its reactivities with O_2, H_2, and CO_2 at temperatures up to 600 °C and created an end-group-protection strategy to stablize it. These observations open a new door to the chemistry of atomic materials.

An exciting development has been witnessed from 3D bulk materials through 2D layer materials to the next-generation 1D chain materials.[1, 2] The sp-hybridized carbon chain (carbyne) is the most promising 1D atomic material, which was proposed as early as 1921.[3] The sp-hybridized atomic orbitals lead to a linear arrangement of carbon atoms with two possible structures as polyyne (with bond length alternation) and cumulene (with equal bond length).[4-7] Owing to Peierls distortion, (semiconductive) polyyne is believed more stable than (metallic) cumulene.[4] So far, most of the synthesized carbon chains possess the polyynic structure,[8-11] while the preparation of cumulene is more challenging especially for long chains.[12]

Based on the bond order theory proposed by Pauling, since carbon atom has 4 unpaired electrons, the total order of the bonds connecting one carbon atom is equal to 4.[13-15] In the past century, polyyne is typically believed to consist of alternating single and triple bonds, while cumulene shows serial double bonds.[4] It is reasonable that the bond order of cumulene is 2 (as a half of 4), whereas the bond orders of the stable structure of polyyne are questionable due to the π-electron delocalization (conjugation). Furthermore, the energy difference between the stable polyyne and cumulene is less than 200 meV per carbon atom,[4, 16] implying that they might be mutually transformed with undergoing a series of intermediate structures with various bond-order pairs whereas the experimental demonstration is still lacking.

More importantly, sp-hybridized carbon chain stands out from other carbon allotropes due to its unique chemical properties resulting from its 1D atomic structure and electron-rich unsaturated bonds.[4] In general, carbon materials can be oxidized into CO and/or CO_2,[17, 18] and carbon allotropes containing sp- and/or sp^2-hybridized carbon (such as carbon nanotube, graphene, and graphyne) can undergo hydrogenation to form sp^3-hybridized carbon.[19-21] The investigation on the chemical reactivity of atomic carbon chains under oxidizing and reducing conditions is highly desirable for their efficient synthesis, safe storage, and promising applications. Furthermore, the end group of atomic carbon chains is believed to play a key role to stabilize the chains despite its small proportion (especially in long chains),[9, 10] whereas the strategy to protect the end group remains unexplored. Herein, focusing on these critical issues, we unprecedentedly report the bond order identification, reversible structural transition (π-electron delocalization), and chemical reactivity of carbon chains, which paves a new avenue for the investigation and application of the state-of-the-art 1D atomic carbon materials.

Referring to previous reports,[11, 22, 23] we prepared sp-hybridized carbon chains *via* the dehydrohalogenation reaction of polyvinylidene fluoride (PVDF) with sodium amide ($NaNH_2$) in high vacuum at high temperature (**Eq. 1**).

$$\{CH_2\text{-}CF_2\}_n + 2n\ NaNH_2 \rightarrow \{C\equiv C\}_n + 2n\ NaF + 2n\ NH_3 \quad (1)$$

This reaction was confirmed by X-ray diffraction (**Fig. S1**) that reveals the disappearance of PVDF and $NaNH_2$ reactants and the generation of NaF. Furthermore, as-produced carbon chains can be purified from NaF and other carbon materials by dissolving in ethanol with a yield of 3.7 wt%.[8, 24] The Fourier-transform infrared (FT-IR) spectrum of the ethanol solution (**Fig. S2**) shows

[a] Department of Materials Science and Engineering, Michigan Technological University, Houghton, Michigan 49931, United States
[b] Center for Functional Nanomaterials, Brookhaven National Laboratory, Upton, New York 11973, United States
Electronic Supplementary Information (ESI) available: [details of any supplementary information available should be included here]. See DOI: 10.1039/x0xx00000x

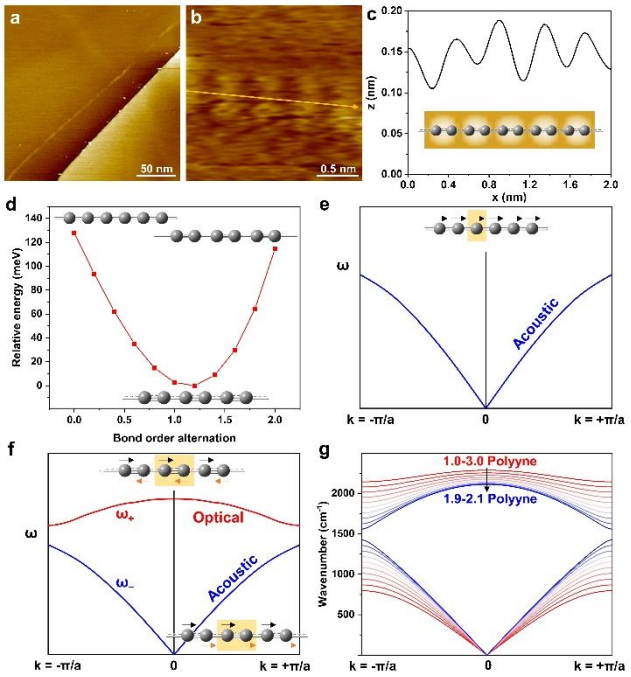

Fig. 1 (a) Low-resolution and (b) high-resolution constant-current STM images of atomic carbon chain at room temperature. (c) Height profile along the yellow arrow in Fig. 1b and simulated STM image (inset). (d) Relation between energy and bond order alternation of atomic carbon chain obtained from DFT calculations. Schematic longitudinal phonon dispersion branch(es) of (e) cumulene and (f) polyyne. (g) Relation between phonon wavenumber and wave vector of carbon chains with varied bond-order pairs.

an intense FT-IR signal at 2168 cm^{-1} which provides strong evidence for the stretching vibration of C≡C bonds,[8] indicating the successful dehydrohalogenation of PVDF towards polyynic carbon chains.

The morphology of carbon chains was identified by ultrahigh-vacuum scanning tunneling microscopy (STM). As shown in **Fig. 1a**, a long linear carbon chain with a length surpassing 307 nm (corresponding to ~2400 carbon atoms) can be clearly resolved on the highly oriented pyrolytic graphite (HOPG) substrate. Furthermore, the high-resolution STM image (**Fig. 1b**) reveals the alternating bright and dark features, implying the alternating electron-rich and electron-deficient bonds of a polyynic carbon chain, which is consistent with the simulated STM image (inset of **Fig. 1c**) and FT-IR result (**Fig. S2**). The height of the chain is approximately 0.15 nm, demonstrating that there is only one carbon atom in the vertical direction (**Fig. 1c**). The slightly larger lateral size of the chain (around 0.5 nm) than the ideal atomic carbon chain is due to the limitation of the lateral resolution of STM by the tip apex size[25, 26] and the poor conductivity of polyynic carbon chains.[9]

Although the polyynic structure of carbon chains has been demonstrated here, it remains a mystery for decades if the bond length alternation of polyyne can be gradually eliminated to form cumulene. Firstly, we conducted density functional theory (DFT) calculations to find the stable structure of cumulene (using a monoatomic unit cell) and polyyne (using a diatomic unit cell). As summarized in **Table S1**, cumulene has an identical bond length of 1.26 Å while polyyne possesses alternating bond lengths of 1.20 Å and 1.35 Å which are consistent with previous experimental and theoretical studies.[27, 28] To figure out the bond order, we built a set of equations (**Eqs. 2-5**) using the Pauling correlation between bond order (n) and bond length (L) and the bond order conservation principle.[13]

$$n_c = e^{\frac{L_0 - L_c}{b}} \quad (2)$$

$$n_{p1} = e^{\frac{L_0 - L_{p1}}{b}} \quad (3)$$

$$n_{p2} = e^{\frac{L_0 - L_{p2}}{b}} \quad (4)$$

$$2 \times n_c = n_{p1} + n_{p2} = 4 \quad (5)$$

where n_c and L_c are the bond order and bond length of cumulene, $n_{p(1,2)}$ and $L_{p(1,2)}$ are the bond order and bond length of polyyne, and L_0 and b are two constants. Plugging in the bond lengths acquired from DFT calculations, we could get the bond order-bond length correlation (**Eq. 6**) and values of n_{p1} (1.4) and n_{p2} (2.6). This demonstrates that the stable polyynic structure has alternating bond orders of 1.4 and 2.6 (denoted as 1.4-2.6 polyyne) instead of the generally-believed 1.0 and 3.0 (denoted as 1.0-3.0 polyyne).

$$n = e^{\frac{1.4383 - L}{0.2558}} \quad (6)$$

Moreover, the energy of cumulene was found 128 meV (per atom) higher than that of 1.4-2.6 polyyne (**Table S1**), revealing that the 1.4-2.6 polyyne is more energetically favorable than cumulene. Further, we calculated the energies of carbon chains with varied bond-order pairs based on the bond order conservation principle (*e.g.*, n_1 = 1.1 and n_2 = 2.9). Clearly, as illustrated in **Fig. 1d**, the energy of carbon chain gradually decreases with increasing bond order alternation (BOA = $n_2 - n_1$) from 0 (for cumulene) to 1.2 (for 1.4-2.6 polyyne) followed by a rise with BOA from 1.2 to 2.0 (for 1.0-3.0 polyyne). Namely, here, the energetical favorability (stability) of 1.4-2.6 polyyne (with regards to the widely-accepted stable structures of cumulene and 1.0-3.0 polyyne) is reported for the first time. Nevertheless, the energy differences among these structures are very small (below 128 meV), suggesting the highly possible structural transition of carbon chains with additional thermal input.

In-situ diffuse reflectance infrared Fourier transform spectroscopy (DRIFTS) is a powerful tool that enables the real-time detection of carbon chain structure at varied temperatures, which is supported by the following theory. As shown in **Fig. 1e**, cumulene (with a monoatomic unit) only shows one acoustic phonon branch along the longitudinal direction corresponding to the in-phase movement of all atoms (overall translation of carbon chain).[29] In contrast, polyyne (with a diatomic unit) possesses one more optical phonon branch along the longitudinal direction which is attributed to the out-of-phase movement of adjacent atoms (**Fig. 1f**) whose vibration frequency lies in the IR region.[4, 29] The dispersion relation in polyynic carbon chain can be expressed as **Eq. 7**[29] in which the force constant (k_1 and k_2) is dependent on the bond order (n) and bond length (L) (**Eq. 8**).[30] Furthermore, the wavenumber of the vibration signal ($\overline{\nu}$) that is detectable by FT-IR spectroscopy can be estimated at the long-wavelength limit (k = 0) (**Eq. 9**).

$$\omega_{\pm} = \sqrt{\frac{k_1 + k_2}{m} \pm \frac{\sqrt{k_1^2 + k_2^2 + 2k_1k_2\cos(ka)}}{m}} \quad (7)$$

$$k_{1,2} = i \times n_{1,2}^2 \times L_{1,2} \quad (8)$$

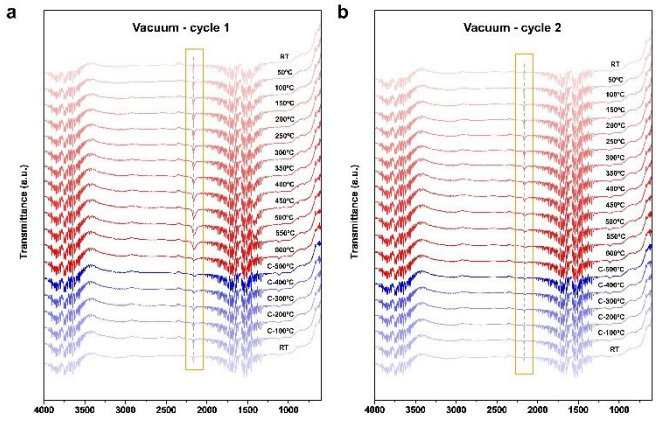

Fig. 2 *In-situ* DRIFTS spectra of carbon chains on KBr substrate in vacuum. (a) The first and (b) the second cycles of heating and cooling.

$$\overline{v} = \frac{\omega_{+0}}{2\pi c} = \frac{\sqrt{\frac{2(k_1+k_2)}{m}}}{2\pi c} \quad (9)$$

where ω, m, k, a, c, and i are the angular frequency, mass of carbon, wave vector, unit cell length, light speed, and a constant (0.8) fitted by the experimentally-acquired wavenumber of the vibration signal. Therefore, the relation between phonon wavenumber and wave vector of carbon chains with varied bond-order pairs can be derived as shown in **Fig. 1g**. It is clear that with the decreasing BOA from 2.0 to 0.2 (from 1.0-3.0 polyyne to 1.9-2.1 polyyne), the optical phonon branch shifts to lower wavenumbers while the acoustic phonon branch shifts to higher wavenumbers. Moreover, the influence of BOA near the long-wavelength limit ($k = 0$) is less significant than that near the first Brillouin zone boundary ($k = \pm \pi/a$). Focusing on the wavenumber at the long-wavelength limit as an approximation for FT-IR vibration signal, a signal downshift from 2288 cm^{-1} through 2168 cm^{-1} to 2113 cm^{-1} would be expected for the transition from 1.0-3.0 polyyne through 1.4-2.6 polyyne to 1.9-2.1 polyyne. Namely, electron delocalization leads to the downshift of vibration signal and the completely homogenous electron distribution (cumulene) causes the disappearance of vibration signal.

To confirm our hypothesis that atomic carbon chain would undergo structural transition with thermal input, we dropped the ethanol solution of carbon chains onto a potassium bromide (KBr) disk, which was then pretreated by high-vacuum annealing to remove ethanol and any adsorbed impurities, leaving carbon chains dispersed on KBr surface. Afterwards, carbon chains were slowly heated at 2 °C/min under vacuuming with continuously recording the DRIFTS signals. Interestingly, as shown in **Fig. 2a**, the stretching vibration signal of carbon chains at 2168 cm^{-1} was significantly weakened and broadened to lower wavenumbers with increasing temperature up to 600 °C but became stronger and sharper again during the cooling process. This trend was further confirmed in the second cycle of heating and cooling (**Fig. 2b**). Here, the temperature-induced reversible change of the vibration signal is attributed to the structural transition of carbon chains resulting from electron delocalization/localization. Namely, while a relatively low temperature is favored for the polyynic structure of carbon chains with a relatively high electron localization degree, a high temperature with increasing kinetic energy for the chains leads to electron delocalization and thus the decreased bond order alternation. At 600 °C, the onset of the vibration signal peak is about 2102 cm^{-1} (below 2113 cm^{-1} for 1.9-2.1 polyyne), implying the existence of polyynic structures that are infinitely close to cumulene. This further, for the first time, demonstrates the trend of polyyne-cumulene transition at high temperatures. Nevertheless, such a heating-cooling treatment destroyed some carbon chains as suggested by the weaker signal after treatment than the initial one (**Table S2**).

The destruction of carbon chains might be due to the instability resulting from the loss of nitrogen end groups (≡N) at high temperatures. The nitrogen end groups were derived from $NaNH_2$ reactant and might help to guide the dehydrohalogenation of PVDF toward polyyne instead of cumulene. To confirm this, we conducted *in-situ* DRIFTS measurements for carbon chains under 10 mL/min N_2 gas flow. As expected, the temperature-induced change of the vibration signal at 2168 cm^{-1} became fully reversible without signal attenuation after cooling (**Fig. 3a**), providing solid evidence for the reversible structural transition (π-electron delocalization-localization) of carbon chains. The negligible carbon chain destruction is due to the suppressed forward-reaction (promoted backward-reaction) of carbon chains to lose end groups (**Eq. 10**) in the presence of N_2. In contrast, the fast removal of N_2 by vacuuming (or under other gas flows) would push this reversible reaction forward and the resulting unsaturated carbon chains are too reactive to retain on KBr substrate.[4, 10] Nitrogen was indeed detected by elemental analysis with a small N:C atomic ratio of 0.002. This suggests as-prepared carbon chains are in the molecular formula of $C_{1000}N_2$, so the average length of carbon chains is 127 ± 1 nm. More importantly, this practice provides a new and efficient approach to protect carbon chains by supplying the end-group-related species.

$$C_nN_2 \leftrightarrow C_n + N_2 \quad (10)$$

The powerful *in-situ* DRIFTS also enables us to examine the chemical reactivity of carbon chains. H_2 is a promising species to react with carbon chains by converting −C≡C− into −HC=CH− and even $-H_2C-CH_2-$. Surprisingly, carbon chains showed a very weak reactivity with H_2 even at 600 °C as demonstrated by the following two aspects. On the one hand, the characteristic signals for C=C, sp^2 C-H, and sp^3 C-H did not emerge (**Fig. 3b**).

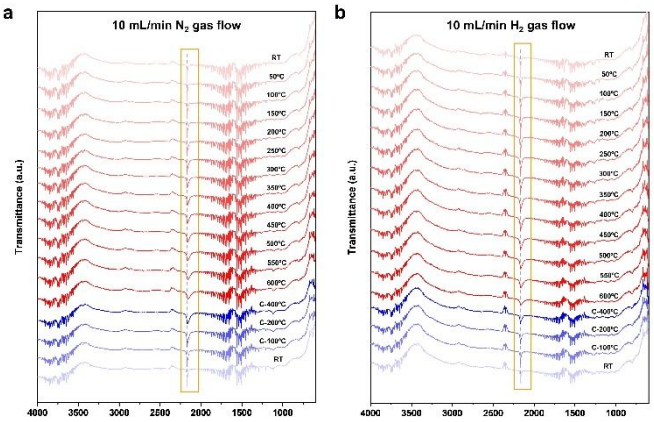

Fig. 3 *In-situ* DRIFTS spectra of carbon chains on KBr substrate under gas flows. (a) N_2 gas flow. (b) H_2 gas flow.

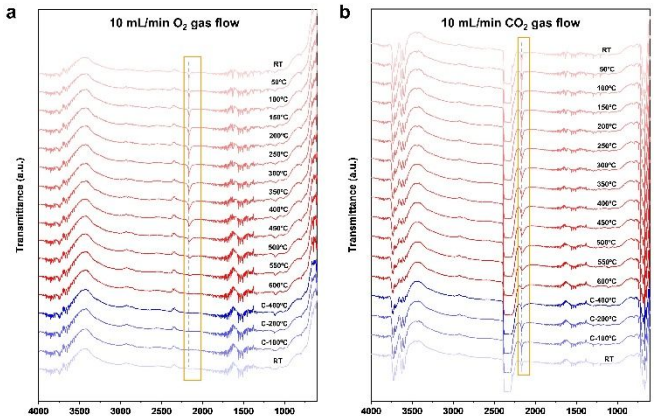

Fig. 4 *In-situ* DRIFTS spectra of carbon chains on KBr substrate under oxidizing conditions. (a) O_2 gas flow. (b) CO_2 gas flow.

On the other hand, for the stretching vibration of carbon chains, a similar phenomenon of signal dispersion during heating and signal intensification during cooling with a similar attenuation degree (42%) to that in vacuum (42~44%) was noticed, implying a similar process of structural transition and end-group destruction. Therefore, carbon chains exhibit a good resistance to hydrogenation at temperatures up to 600 °C, which agrees well with graphene and carbon nanotubes, while the application of high pressures (5~10,000 MPa) might help with the hydrogenation.[19, 20]

Furthermore, the reactivities of carbon chains with oxidizing gases O_2 and CO_2 were evaluated. Under O_2 flow, the intensity of the carbon chain stretching vibration signal decreased with increasing temperature and disappeared at 600 °C, which could not be resumed during the cooling process (**Fig. 4a**). This indicates carbon chains can be fully oxidized by O_2 at 600 °C, in good agreement with other carbon materials that became intensively oxidized at temperatures over 500 °C.[17] Moreover, CO_2 is a milder oxidant for carbon materials in comparison to O_2, driving the comproportionation reaction with forming CO at elevated temperatures. As shown in **Fig. 4b**, the carbon chain stretching vibration signal was weakened with increasing temperature and then strengthened while cooling. The attenuation degree of the signal after heating-cooling treatment is 47%, which is slightly larger than that in vacuum (42~44%), suggesting that a small amount of carbon chains reacted with CO_2 at temperatures up to 600 °C. The reactivity of carbon chains with CO_2 is similar to those of graphene and carbon nanotubes with partial oxidation to create surface micropores and/or defects.[31, 32]

In summary, we have unprecedentedly demonstrated the structural transition and chemical reactivity of sp-hybridized carbon chains. The energetically favorable structure of carbon chain has alternating bond orders of 1.4 and 2.6 rather than the generally-believed 1.0 and 3.0. Moreover, the electron delocalization of carbon chains toward a more homogeneous structure occurred upon heating, which could be reversed during the cooling process. Besides, carbon chains exhibited a good resistance to H_2 and CO_2 even at high temperatures up to 600 °C, while showing a high reactivity with O_2. Furthermore, we demonstrated an efficient strategy to achieve an excellent stability of carbon chains by protecting the end groups under N_2 atmosphere. These results offer the opportunity to boost the development of sp-hybridized atomic carbon materials.

Conflicts of interest

There are no conflicts to declare.

Notes and references

1. X. Pang, Y. He, J. Jung and Z. Lin, *Science*, 2016, **353**, 1268-1272.
2. T. Li, C. Chen, A. H. Brozena, J. Y. Zhu, L. Xu, C. Driemeier, J. Dai, O. J. Rojas, A. Isogai, L. Wågberg and L. Hu, *Nature*, 2021, **590**, 47-56.
3. G. Tammann, *Z. Anorg. Allg. Chem.*, 1921, **115**, 145-158.
4. C. S. Casari, M. Tommasini, R. R. Tykwinski and A. Milani, *Nanoscale*, 2016, **8**, 4414-4435.
5. Y. H. Hu, *J. Phys. Chem. C*, 2009, **113**, 17751-17754.
6. S. Fang and Y. H. Hu, *Carbon*, 2021, **171**, 96-103.
7. Y. H. Hu, *J. Phys. Chem. C*, 2011, **115**, 1843-1850.
8. B. Pan, J. Xiao, J. Li, P. Liu, C. Wang and G. Yang, *Sci. Adv.*, 2015, **1**, e1500857.
9. Y. Gao, Y. Hou, F. Gordillo Gámez, M. J. Ferguson, J. Casado and R. R. Tykwinski, *Nat. Chem.*, 2020, **12**, 1143-1149.
10. W. A. Chalifoux and R. R. Tykwinski, *Nat. Chem.*, 2010, **2**, 967-971.
11. A. J. Dias and T. J. McCarthy, *J. Polym. Sci. Polym. Chem. Ed.*, 1985, **23**, 1057-1061.
12. M. Franz, J. A. Januszewski, D. Wendinger, C. Neiss, L. D. Movsisyan, F. Hampel, H. L. Anderson, A. Görling and R. R. Tykwinski, *Angew. Chem. Int. Ed.*, 2015, **54**, 6645-6649.
13. L. Pauling, *J. Am. Chem. Soc.*, 1947, **69**, 542-553.
14. Y. H. Hu, *J. Am. Chem. Soc.*, 2003, **125**, 4388-4390.
15. Y. H. Hu and E. Ruckenstein, *J. Am. Chem. Soc.*, 2005, **127**, 11277-11282.
16. Y. H. Hu, *Phys. Lett. A,* 2009, **373**, 3554-3557.
17. V. Z. Shemet, A. P. Pomytkin and V. S. Neshpor, *Carbon*, 1993, **31**, 1-6.
18. Z. Sun and Y. H. Hu, *Acc. Mater. Res.*, 2021, **2**, 48-58.
19. Y. Fei, S. Fang and Y. H. Hu, *Chem. Eng. J.*, 2020, **397**, 125408.
20. A. V. Talyzin, S. Luzan, I. V. Anoshkin, A. G. Nasibulin, H. Jiang, E. I. Kauppinen, V. M. Mikoushkin, V. V. Shnitov, D. E. Marchenko and D. Noréus, *ACS Nano*, 2011, **5**, 5132-5140.
21. Y. H. Hu and E. Ruckenstein, *J. Chem. Phys.*, 2005, **123**.
22. S. E. Evsyukov, Y. P. Kudryavtsev and Y. V. Korshak, *Russ. Chem. Rev.*, 1991, **60**, 373-390.
23. Y. P. Kudryavtsev, N. A. Bystrova and L. V. Zhirova, *Russ. Chem. Bull.*, 1996, **45**, 2237-2239.
24. H. Tabata, M. Fujii and S. Hayashi, *Carbon*, 2006, **44**, 522-529.
25. F. Hui, C. Wen, S. Chen, E. Koren, R. Dechter, D. Lewis and M. Lanza, *Adv. Funct. Mater.*, 2020, **30**, 1902776.
26. S. Fang and Y. H. Hu, *Matter*, 2021, **4**, 1189-1223.
27. K. Kaiser, L. M. Scriven, F. Schulz, P. Gawel, L. Gross and H. L. Anderson, *Science*, 2019, **365**, 1299-1301.
28. M. Liu, V. I. Artyukhov, H. Lee, F. Xu and B. I. Yakobson, *ACS Nano*, 2013, **7**, 10075-10082.
29. G. Burns, *Solid state physics*, Academic press, 2016.
30. P. Politzer and S. Ranganathan, *Chem. Phys. Lett.*, 1986, **124**, 527-530.
31. D. Wang, K. Wang, H. Wu, Y. Luo, L. Sun, Y. Zhao, J. Wang, L. Jia, K. Jiang, Q. Li, S. Fan and J. Wang, *Carbon*, 2018, **132**, 370-379.
32. L. Chang, D. J. Stacchiola and Y. H. Hu, *ACS Appl. Mater. Interfaces,* 2017, **9**, 24655-24661.